Available online at www.sciencedirect.com
SCIENCE DIRECT®
International Journal of Heat and Mass Transfer 47 (2004) 3233–3244
International Journal of HEAT and MASS TRANSFER
www.elsevier.com/locate/ijhmt

# Performance analysis of the transient thermo-reflectance method for measuring the thermal conductivity of single layer materials

Pavel L. Komarov, Peter E. Raad *

*Department of Mechanical Engineering, Southern Methodist University, Dallas, TX 75275-0337, USA*

Received 17 October 2003; received in revised form 6 February 2004
Available online 16 March 2004

**Abstract**

This work shows that the Fourier number (*Fo*) defines the shape and amplitude of the thermal response of a semi-infinite layer sample. The introduction of the responsivity, Rs, of the TTR method provides the ability to assess the performance of the thermal conductivity measurements. A simplified heat transfer analysis of a finite layer sample revealed that the properties ratio, $(\rho C_p K)_S/(\rho C_p K)_L$, and the layer thickness, $h/\delta_P$, uniquely define both temperature response and measurement responsivity. If the material under test is the substrate, this work can help improve the measurement accuracy by selecting the appropriate thickness of the top layer. If the material is a layer on top of a known substrate, this work suggests that the accuracy of the TTR measurements can be fully maximized.


*Keywords:* Transient thermo-reflectance; Thermal conductivity measurements; Uncertainty minimization; TTR performance

## 1. Introduction

The high rate of innovation in the electronics and telecommunications fields has raised expectations for increased performance and functionality. Most advances have evolved from smart engineering and efficient manufacturing practices. Equally substantial gains, however, can be made from the introduction of innovative materials. Indeed, miniaturization and performance requirements have forced the use of existing materials beyond initially envisioned ranges and have spurred the development of special materials [1]. Knowledge of material properties is fundamental to the design process, especially for electronic and telecommunication devices, where performance depends heavily on electro-thermal interactions.

Higher performance is only possible by significant reductions in the size of active features, which in turn can increase heat generation densities to critical levels. With the use of submicron devices came the realization that bulk and thin-film thermal properties differ markedly [2]. However, since no universal behavior is expected for these differences and since they cannot be predicted from theory [3], the properties of each material must be measured individually. Also, as films are typically layered and deposition techniques differ by manufacturer, it is important to measure the interface resistance of stacked layers [4].

The transient thermo-reflectance method (TTR) [5] is preferred among the various experimental techniques [6] used to determine the thermal conductivity of thin-film and multi-layered materials. The main advantage of the TTR method is that it is a non-contact and non-destructive optical approach, both for heating a sample under test and for probing the variations of its surface temperature [7]. Because the method is non-invasive, it is attractive for the measurement of the thermal properties of thin-layer materials whose investigation by invasive

* Corresponding author. Tel.: +1-214-768-3043; fax: +1-214-768-4998.
*E-mail addresses:* pavel@engr.smu.edu (P.L. Komarov), praad@smu.edu, praad@mail.smu.edu (P.E. Raad).

0017-9310/$ - see front matter © 2004 Elsevier Ltd. All rights reserved.
doi:10.1016/j.ijheatmasstransfer.2004.02.006

**Nomenclature**

| | |
|---|---|
| $Fo$ | Fourier number, $Fo = \alpha\tau/\delta_\lambda^2$ |
| $F$ | fluence of heating laser irradiation |
| $h$ | thickness of a layer |
| $h^*$ | minimal thickness of a *semi-infinite* layer |
| $I(t)$ | heating irradiation intensity, Eq. (3) |
| $k$ | extinction coefficient of a sample material |
| $K$ | thermal conductivity of a sample material |
| $Q_{ab}(z,t)$ | laser energy absorbed by a sample |
| $R$ | reflectivity of a sample surface |
| Rs | responsivity of the TTR measurement of K |
| $t$ | time |
| $t_0$ | time at which heating laser intensity reaches its maximum value |
| $T$ | non-dimensional time, $T = t/\tau$ |
| $T_{0.1}(a)$ | non-dimensional time at which $\widetilde{\Theta} = 0.1$ |
| $z$ | coordinate that is normal to a sample surface |
| $Z$ | non-dimensional coordinate, $Z = z/\delta_\lambda$ |
| *Greek symbols* | |
| $\alpha$ | thermal diffusivity of a sample material, $\alpha = K/(\rho C_p)$ |
| $\gamma$ | absorption coefficient of a sample material, $\gamma = 4\pi k/\lambda$ |
| $\delta_\lambda$ | light penetration depth of a heating laser, $\delta_\lambda = 1/\gamma$ |
| $\delta_P$ | heat penetration depth during a cycle of heating laser pulse, $\delta_P = \sqrt{\alpha\tau}$ |
| $\delta_H$ | heat penetration depth of the laser pulse energy into a sample while $\widetilde{\Theta} \geqslant 0.1$ |
| $\Phi$ | ratio of substrate and layer material properties, $\Phi = (\rho C_p K)_S/(\rho C_p K)_L$ |
| $\theta$ | temperature of a sample |
| $\theta^*$ | reference temperature, $\theta^* = F/(\rho C_p \delta_\lambda)$ |
| $\Theta$ | non-dimensional temperature of a sample, $\Theta(Z,T) = \theta(Z,T)/\theta^*$ |
| $\widetilde{\Theta}$ | normalized temperature of a sample surface, $\widetilde{\Theta}(T) = \Theta(0,T)/\Theta_{max}$ |
| $\lambda$ | wavelength of a heating laser |
| $\rho C_p$ | specific heat of a sample material |
| $\sigma_{Fo}$ | measurement uncertainty of $Fo$ number |
| $\sigma_{\widetilde{\Theta}}$ | measurement uncertainty of a normalized temperature |
| $\tau$ | pulse width of a heating laser |

methods would present the difficulties of having to fabricate a measuring device into a sample, and then having to isolate and exclude the influence of the measuring device itself.

The basic principle of the transient thermal reflectance method is to heat a sample by laser irradiation and probe the changes in the surface reflectivity of the heated material. The schematic in Fig. 1(a) depicts the square heating and round probing spots produced by the TTR system built by the authors at SMU (http://engr.smu.edu/netsl). The source of energy in the TTR method is normally provided by a pulsed laser with short pulse duration. During each pulse, a given volume on the sample surface heats up to a temperature level above ambient due to the laser light energy absorbed into the sample. The heating area is specified by adjusting the pulsing laser aperture and the optics of the system. The depth of the volumetric heating, on the other hand, is determined by the optical penetration depth, which is a function of laser wavelength and surface material properties. The heating level through the light penetration depth ($\delta_\lambda$) obeys an exponential decay law, as described later. After each laser pulse is completed, the sample begins to cool down to the initial ambient temperature. During this process, the probing CW laser light reflected from the sample surface at the heating spot center (probing spot in Fig. 1(a)) is collected on a

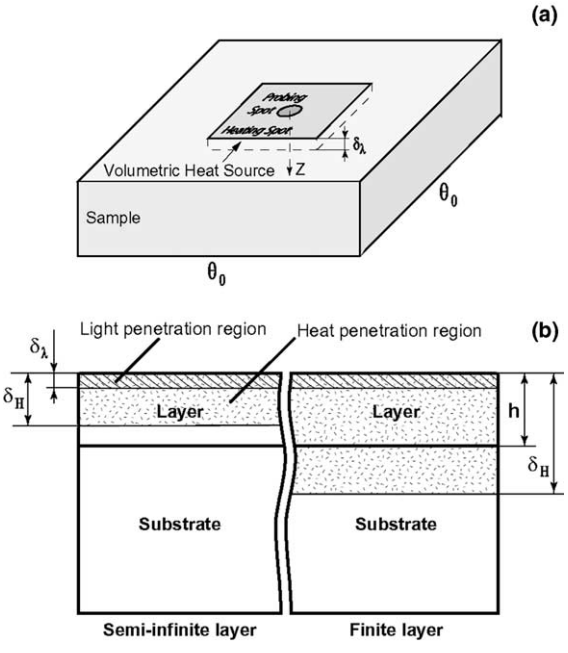


Fig. 1. Problem geometry and important parameters: (a) heating and probing spots on a sample; and (b) different heat penetration depths imply either semi-infinite or finite layer behavior.

photodetector that reads the instantaneous surface reflectivity. The changes in surface reflectivity are linearly proportional to the changes in surface temperature, within a wide but finite temperature range [8].

The influence of a pulsed laser irradiation on a given material depends both on the optical properties of that material as well as on the wavelength and pulse duration of the laser itself. Thus, the wavelength and pulse width are important parameters in the determination of the effectiveness of the TTR method for different materials. Although several articles in the literature address the application of the TTR method for different stacked materials [9], a systematic investigation of the influence of the laser wavelength and pulse width on the performance of the method has not yet been presented even for the simplest bulk material measurements.

Before proceeding, it is important to define what is meant by *bulk* material. Traditionally, a bulk sample, as opposed to a *thin-film* sample, has been used to denote a piece of material that is large enough for its size not to affect its thermal conductivity. In contrast, a thin-film sample has at least one of its dimensions in the submicron range and its thermal conductivity ($K$) is dependent on the size of that smallest dimension (normally $K$ decreases as the sample gets thinner) [2]. The bulk and thin-film terms qualitatively characterize sample material properties in terms of the atomic structure of the material and the dimensions of the sample. As shown by Cahill [2] the thickness of the thin-film should be less than 10 times that of the mean free path of the energy carriers of the thin-film material. The differentiation between bulk and thin-film is of practical importance because the heat transfer mechanism in thin-films is influenced by boundary effects on the energy carriers, and, as a result, is governed by a more complex heat transfer equation and requires more effort for analysis than that in bulk. With an ultimate target of investigating thin-film samples, this work is concerned with the necessary first step of assessing the performance and determining the range of applicability of the TTR method only for bulk materials.

In addition to the bulk and thin-film definitions, two other terms, *semi-infinite* and *finite* layers are introduced here to characterize the behavior of layers of a sample in the context of the TTR method (See Table 1 and Fig. 1(b)). Samples of interest are often formed by one or more layers of different materials deposited on the substrates. Since the TTR method depends on heating a sample under test with a pulsed laser of a specific pulse width, the method has a characteristic time associated with the duration of the temperature response within the sample. This transient nature of the TTR method in turn justifies considering a layer of sample as semi-infinite or finite layer. Specifically, if the overall heat penetration process experienced during a measurement cycle only partially involves a particular layer of the sample, this layer can be considered as a semi-infinite layer, irrespective of the structure of the underlying part (left side of Fig. 1(b)). If, on the other hand, the heat energy penetrates entirely through a layer, it becomes imperative to take into account the thermal properties of the material making up the affected layer as well as the interface resistance between this layer and its neighbors. As such, the layer of the sample should be classified as a finite layer (right side of Fig. 1(b)). Additional details of the approach to classifying samples will be given later.

Table 1
Classification of material samples based on the ratio between the heat penetration depth and the thickness of the top layer

| Thermal conductivity behavior | Transient temperature response behavior | |
|---|---|---|
| | Semi-infinite layer | Finite layer |
| Bulk | (I) $K = \text{const}$; $h > \delta_H$ | (II) $K = \text{const}$; $h < \delta_H$ |
| Thin-film | (III) $K = f(h)$; $h > \delta_H$ | (IV) $K = f(h)$; $h < \delta_H$ |

The ultimate impact of this work would be to extend the TTR approach for the non-destructive measurement of the thermal properties of new and existing multi-layered materials, including metals, semiconductors, and dielectrics. However, in this first step, the investigation will focus on applying the TTR method to the measurement of the thermal conductivity of bulk samples having single semi-infinite or finite layers on the substrate, assuming that the effects of the interface resistance between them are negligible; future work will incorporate this additional complexity. This first step will make it possible to determine the method's range of applicability, to establish the criterion for distinguishing between semi-infinite and finite layers on the basis of an analytical solution of the governing heat transfer system, and to assess the performance of the TTR method for the type of layers mentioned above.

## 2. Heat transfer modeling

The TTR method is useful and applicable for a wide range of time scales from femtosecond to microsecond. However, in the femtosecond regime, the governing physics cannot be described by the Fourier equation because the heat absorption process involves two stages, namely, photon–electron interactions in the first hundreds of femtoseconds and electron–phonons thereafter [10]. In this work, the focus is on the range where the Fourier equation is applicable, which implies a range of heating pulse widths on the order of tens of picoseconds and above.

Given that the characteristic dimension of the (uniformly) heated spot is much larger than both the probing spot and the heat penetration depth during a measurement, it is acceptable to describe the physical problem with the one-dimensional heat equation [11],

$$\rho C_p \frac{\partial \theta}{\partial t} = \frac{\partial}{\partial z}\left(K \frac{\partial \theta}{\partial z}\right) + Q_{ab}(z,t) \tag{1}$$

The top surface of the sample is considered adiabatic, i.e., $\partial\theta/\partial z = 0$ at $z = 0$; the bottom surface is held isothermal by contact with the chuck, i.e., $\theta = \theta_0$ as $z \to \infty$; and the sample is initially at a uniform temperature, i.e., $\theta = \theta_0$ at $t = 0$. In this work, $K$ is assumed to vary mildly within the temperature ranges considered in the TTR approach.

In the TTR method, the energy source term, $Q_{ab}(z,t)$, represents heating due to optical absorption, which follows an exponential decay within the material [12],

$$Q_{ab}(z,t) = I(t)(1-R)\gamma e^{-\gamma z} \tag{2}$$

$$I(t) = \frac{2F}{\tau\sqrt{\pi}} e^{-4((t-t_0)/\tau)^2} \tag{3}$$

Eqs. (1)–(3) are applicable to both semi-infinite and finite layer samples. However, the complexity of their solutions for a finite layer sample is much higher than that for a semi-infinite layer sample. Taking this into account, the heat transfer problem for the former case has been solved with a numerical simulation, while the latter case has been solved analytically with a numerical estimation of the integrals of the final expression. Both approaches are presented next.

### 2.1. Semi-infinite layer sample

Considering the semi-infinite layer sample as a uniform bulk material, the thermal conductivity temperature independent, and $\theta_0$ equal zero, the surface temperature solution [13] appears as:

$$\theta(z,t) = \frac{\alpha}{K}\int_0^t \frac{1}{\sqrt{4\pi\alpha(t-t')}} \int_0^\infty Q_{ab}(z',t') \cdot \left(\exp\left(\frac{-(z-z')^2}{4\alpha(t-t')}\right) + \exp\left(\frac{-(z+z')^2}{4\alpha(t-t')}\right)\right) dz'\,dt' \tag{4}$$

Since in the TTR method only the surface temperature can be detected, it is reasonable to simplify the equation above for the case of $z = 0$, which yields

$$\theta(0,t) = \frac{\alpha}{K}\int_0^t \frac{1}{\sqrt{\pi\alpha(t-t')}} \int_0^\infty Q_{ab}(z',t') \cdot \exp\left(\frac{-z'^2}{4\alpha(t-t')}\right) dz'\,dt' \tag{5}$$

Then, by substituting Eqs. (2) and (3) into Eq. (5), one can obtain the temperature on the sample surface in dimensional form:

$$\theta(0,t) = \frac{2F\gamma}{\pi\tau\sqrt{\rho C_p K}} \int_0^t \frac{\exp\left(-4\left(\frac{t_0-t'}{\tau}\right)^2\right)}{\sqrt{(t-t')}} \times \left(\int_0^\infty \exp\left(-z'\left(\gamma + \frac{z'}{4\alpha(t-t')}\right)\right) dz'\right) dt' \tag{6}$$

By introducing the laser pulse duration, $\tau$, as a time scale, the laser light penetration depth, $\delta_\lambda = 1/\gamma$, as a length scale, and $\theta^* = F/(\rho C_p \delta_\lambda)$ as a temperature scale, it is possible to rewrite the above analytical solution in non-dimensional form, which will facilitate further analysis,

$$\Theta(0,T) \equiv \theta(0,T)/\theta^* = \frac{2}{\pi\sqrt{Fo}} \int_0^T \frac{e^{-4(T_0-T+T')^2}}{\sqrt{T'}} \times \left(\int_0^\infty \exp\left(-Z'\left(1 + \frac{Z'}{4\,Fo\,T'}\right)\right) dZ'\right) dT' \tag{7}$$

where $Fo = \alpha\tau/\delta_\lambda^2$ is the Fourier number. Examples of the temperature response for several values of $Fo$ are shown in Fig. 2(a); the integrals in Eq. (7) have been evaluated numerically.

Since there is only one parameter that defines the surface temperature response of a sample, namely the Fourier number $Fo$, it is important to clarify the physical meaning of this parameter. The square-root of the $Fo$ represents the ratio of the heat penetration depth during a cycle of heating laser pulse and the optical penetration depth of heat laser irradiation. This understanding of the ratio is arrived at by realizing that the thermal penetration depth during a time period $t$ through a medium whose thermal diffusivity is $\alpha$ can be estimated by $\sqrt{\alpha t}$ [12].

### 2.2. Finite layer sample

In the case of a finite layer sample, the analytical approach applied for a semi-infinite layer sample is not beneficial due to the complexity of the solution caused by the jump in the thermal conductivity value at the interface between the layer and the substrate. Thus, a numerical approach is more appropriate for analyzing a finite layer sample [13]. To do so, the heat equation (1) is discretized with central finite differences. A Padé-based three-point-backward scheme has been used for time integration because of its higher accuracy and unconditional stability [14]. The resulting algorithm is second-order accurate in both space and time.

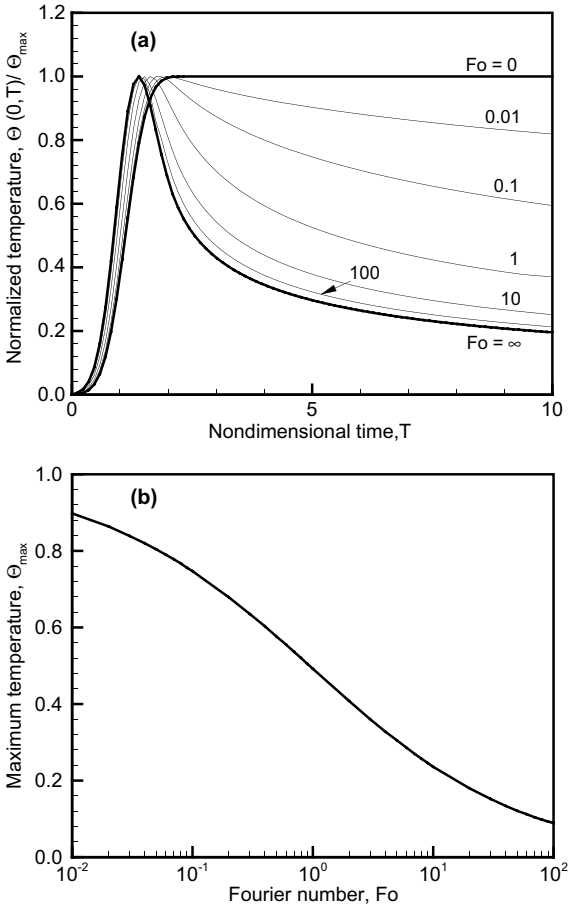


Fig. 2. Influence of *Fo* on temperature response of a semi-infinite layer sample: (a) shape and (b) amplitude.

In order to quantify the accuracy of the numerical simulation, a grid convergence study was conducted by obtaining non-dimensional temperature responses of a representative problem with different values of grid size $\Delta Z$. The problem geometry chosen is a stacked sample consisting of an Si substrate covered with 1 μm of $SiO_2$, which in turn is covered with 1.5 μm of Au. The maximum error relative to the response obtained with the smallest grid spacing, $\Delta Z = 10$ Å, are listed in Table 2 for a range of six larger grid sizes. Since negligible error levels of 0.04% are obtained at $\Delta Z = 20$ Å, all subsequent computations were conducted with a grid size of 10 Å.

## 3. Results and discussion

### 3.1. Semi-infinite layer sample

It is useful to begin by analyzing the less complicated case of a semi-infinite layer sample, i.e., a bulk piece of a given material of interest. The form of Eq. (7) suggests that there are two ways of extracting the unknown thermal conductivity from the measured experimental data. The first approach is based on the dependence of the maximum temperature $\Theta_{\max}$ upon the *Fo* number (Fig. 2(b)); as such, this approach can be referred to as the "amplitude" method. It requires (i) mapping the output of the photodiode signal to the actual temperature response by the use of an independent calibration curve that relates the surface temperature and reflectivity of the sample; (ii) calculating the reference temperature $\theta^*$ with known values of the laser fluence $F$ and $\rho C_p$ of the material under test; and (iii) extracting $K = Fo\,\rho C_p \delta_\lambda^2/\tau$ from the value of *Fo* obtained by the use of the relationship shown graphically in Fig. 2(b). The "amplitude" method appears to be useful only in those cases where the calibration curve is obtained with high accuracy. Unfortunately, the change in material reflectivity is a weak function of changes in surface temperature, namely, around $10^{-4}$–$10^{-5}$ $K^{-1}$, which leads to low accuracy for the calibration curve, and consequently, unsatisfactory uncertainty levels of the "amplitude" approach in most situations.

In order to eliminate these difficulties, many investigators use instead a normalized photodiode response, which can be obtained by dividing the regular output signal by the maximum value of that signal [15]. Given the linear dependence between changes in reflectivity and changes in temperature [16], which holds true for reasonable temperature ranges, a normalized photodiode response would equal a normalized temperature response, avoiding the need for calibration curves and their associated higher levels of uncertainty. Thus, instead of relying on the dependence of the temperature on the *Fo* number, this latter approach deals with the dependence of the response shape, and is hence referred to as the "shape" method. The influence of *Fo* on the normalized temperature response is shown in Fig. 2(a). For a given semi-infinite layer material of known $\rho C_p$ and light penetration depth $\delta_\lambda$, and a given laser with known pulse width $\tau$, it becomes possible to extract the thermal conductivity of that material from $K = Fo\,\rho C_p \delta_\lambda^2/\tau$ by varying *Fo* until the experimental

Table 2
Convergence of the numerical simulation for a stacked sample

| $\Delta Z$ (Å) | 640 | 320 | 160 | 80 | 40 | 20 | 10 |
|---|---|---|---|---|---|---|---|
| Peak error (%) | 7.3 | 3.8 | 1.4 | 0.48 | 0.09 | 0.04 | – |

data and the corresponding analytical solution (Eq. (7)) agree in the RMS sense (in other words, by minimizing the standard deviation, $\sigma_M$, between the measured and calculated temperature responses).

The curves in Fig. 2(a) also suggest that for an acceptable measurement accuracy, the *Fo* number cannot exceed some maximum value. Otherwise, the deviation between the temperature response and the limiting lower curve (i.e., $Fo = \infty$) becomes smaller than the experimental uncertainty of the measurements. Taking into account that measurement accuracy is the most essential characteristic of any experimental method, it is important to analyze in detail the responsivity of the "shape" approach, since responsivity is directly related with the measurement accuracy.

First, the definition of the responsivity of the "shape" approach must be introduced. According to the common definition, the relative responsivity, Rs is $(x \cdot dy)/(y \cdot dx)$, where $y$ is a measured response caused by a specified value of an independent variable $x$. Normally, for the TTR method, $x$ is the thermal conductivity, $K$. However, keeping in mind that in the non-dimensional Eq. (7), $K$ is embedded into *Fo*, the latter can be considered as $x$, while $y$ is the normalized temperature response $\widetilde{\Theta}(T) = \Theta(0,T)/\Theta_{max}$. Since $\widetilde{\Theta}(T)$ is not a single value, but rather a function of time characterized by the capabilities of the experimental setup, it is preferable to define the responsivity Rs of the "shape" approach as $Fo(d\widetilde{\Theta}(T)/dFo)_{max}$ within the time domain specified by the TTR measurement cycle. The results of numerically differentiating Eq. (7) indicate that the responsivity Rs tends to a maximum asymptotic value $Rs_{max} = 0.125$ for low values of *Fo* and decays to zero as $Fo \to \infty$. The behavior of the responsivity Rs as a function of the *Fo* number is shown as a solid curve in Fig. 3(a). The responsivity of the TTR "shape" approach falls below 20% of the maximum value, $Rs_{max}$, at $Fo = 100$, which means that the approach fails for $Fo > 100$. In order to achieve the best responsivity for the method, measurements should be carried out at as small an *Fo* value as practically possible.

The obtained responsivity curve is very helpful for estimating the random measurement uncertainty of the TTR method. Indeed, if some particular TTR measurement system has an apparatus uncertainty, $\sigma_{\widetilde{\Theta}}$ (defined by random deviation of the normalized temperature response from one set to another), and a matching uncertainty, $\sigma_M$ (defined by the TTR fitting procedure), then the measurement uncertainty of the *Fo* number becomes $\sigma_{Fo} = Rs^{-1}\,Max(\sigma_{\widetilde{\Theta}}, \sigma_M)$. For example, the TTR system in the NETS laboratory at SMU has a $\sigma_{\widetilde{\Theta}} \approx 0.0074$, which yields a minimum measurement uncertainty for the thermal conductivity, $K$, of about 6%, assuming that $\sigma_M < \sigma_{\widetilde{\Theta}}$ and that the uncertainties associated with $\rho C_p$, $\delta_\lambda$, and $\tau$ are negligible as compared to $\sigma_{Fo}$. As implied by the dashed line curve in Fig. 3(a), the measurement uncertainty increases with increasing *Fo*. For $Fo > 10$, the measurement uncertainty of the present setup exceeds 15%, which, depending on the application, could be considered as inappropriately high.

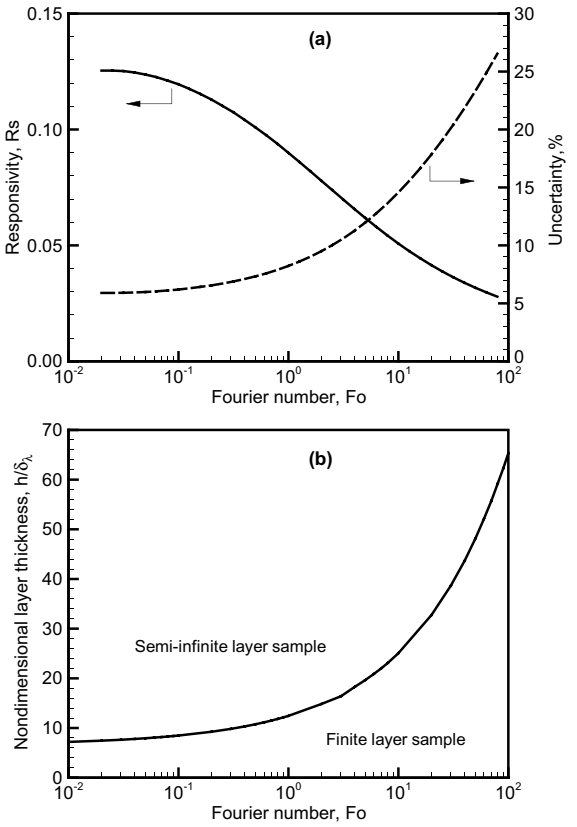


Fig. 3. Influence of *Fo* in the TTR method: (a) responsivity (solid) and measurement uncertainty (dashed); and (b) classification of "semi-infinite layer" and "finite layer" samples.

A key presupposition in the solution of the problem described above is that the top layer of the sample should be thick enough, or, mathematically speaking, it has to be a semi-infinite medium. From a practical point of view, the question becomes "when can a sample under test be considered as a semi-infinite layer sample of a particular material for the characteristics of a given experimental system?" Otherwise, the sample should be considered as having a finite layer, or a stack of finite layers, requiring a different and more complicated solution of the heat transfer problem than that given by Eq. (7) for determining the temperature response. The answer is tied to a specific criterion for the thickness of the top layer, which makes it possible to distinguish the two cases from each other. For this purpose, it is useful to introduce a spatial limitation involving the penetration depth of the laser pulse energy through a sample, $\delta_H$, at which the surface temperature response has nearly disappeared (i.e., $\widetilde{\Theta} = 0.1$). If the depth, $\delta_H$, is smaller than the thickness of

the top layer, $h$, the sample can be considered as a semi-infinite layer sample (see Fig. 1(b)). This criterion combined with the relationship of the heat penetration depth with time, $\delta = \sqrt{\alpha t}$, yields an expression for the limiting thickness that distinguishes the "semi-infinite layer" from the "finite layer" cases; namely,

$$\frac{h^*}{\delta_\lambda} = \sqrt{Fo \cdot T_{0.1}(Fo)} \tag{8}$$

where $T_{0.1}(Fo)$ is the non-dimensional time at which $\bar{\Theta} = 0.1$. The corresponding limiting curve within the $Fo$ range from 0.01 through 100 is provided in Fig. 3(b). All samples with the top layer thickness above the limiting curve are semi-infinite layer samples while those below the curve should be considered as finite layer samples. Increasing the $Fo$ causes the limiting value, $h^*/\delta_\lambda$, to increase. At low values of the $Fo$ number, the limiting thickness asymptotically decreases to $h^*/\delta_\lambda \approx 7$. This fact indicates that the pulsed laser heat energy penetrates into a semi-infinite layer sample by a distance that is at least seven times deeper than the corresponding optical laser irradiation.

Additionally, it should be noted that the above limiting criterion does not depend only on material properties, but also on the laser pulse duration. The important implication is that the same sample can be considered either a semi-infinite layer or a finite layer sample, depending on the heating laser being used. This issue has been well illustrated by the authors of Ref. [12], for example, where the femtosecond TTR method was applied to thin-metal layers (≈100 nm) without any evidence of thermal interaction with the substrate underneath the thin metal.

### 3.2. Finite layer sample

Using the above criterion (Eq. (8)), it is possible to determine if a given sample can be treated as a finite layer case (right side of Fig. 1(b)). If so, then one is more likely to solve the heat transfer problem (Eq. (1)) numerically due to the complexity of the analytical solution for the finite layer sample. The normalized temperature response and the responsivity become functions of the material properties of both the layer and the substrate as well as the geometry of the sample (layer thickness), as opposed to the semi-infinite layer case for which the temperature response and the responsivity are functions of $Fo$ only. However, there is a way to simplify the analysis of the finite layer problem for some cases. Indeed, consider the heat energy accumulated in a sample over a period of time $t$, assuming that $t$ is long enough to allow the heat to propagate through the top layer and into the substrate. For a square unit of the sample surface, the total energy accumulated in the sample under test can be expressed as

$$E(t) = (\rho C_p)_{\mathrm{L}} \int_0^h \theta(t,z)\,\mathrm{d}z + (\rho C_p)_{\mathrm{S}} \int_h^{h+\delta} \theta(t,z)\,\mathrm{d}z \tag{9}$$

Here, the first term is the energy accumulated in the layer while the second term represents the energy accumulated in the substrate. The depth, $\delta$, to which the heat reaches into the substrate can be estimated as $\delta = \sqrt{\alpha_{\mathrm{S}}(t-t')}$, where $t' = h^2/\alpha_{\mathrm{L}}$ is the time required for the heat to propagate through the layer. Now, by applying the integral mean value theorem, $\int_{z_1}^{z_2} \theta(t,z)\,\mathrm{d}z = \bar{\theta}(t)\cdot(z_2 - z_1)$, to the integrals in Eq. (9) and replacing $h$ and $\delta$ with their estimates shown above, it is possible to express the accumulated energy in the following form:

$$E(t) = \sqrt{(\rho C_p K)_{\mathrm{L}} t'}\,\bar{\theta}_{\mathrm{L}}(t) + \sqrt{(\rho C_p K)_{\mathrm{S}}(t-t')}\,\bar{\theta}_{\mathrm{S}}(t) \tag{10}$$

For further analysis, it is reasonable to assume that all laser pulse energy has been absorbed by a time $t_{\max}$ at which $\bar{\theta}_{\mathrm{L}}(t)$ reaches its maximum value $\bar{\theta}_{L\max}$. Hence, for any time $t > t_{\max}$ the equality $E(t) = E(t_{\max})$ holds true, given the reasonable assumption that losses from the surface due to free convection and radiation are negligible. Evaluating Eq. (10) at $t$ and $t_{\max}$, substituting the resulting expressions into the energy equality, and finally dividing the resulting equation by $\sqrt{(\rho C_p K)_{\mathrm{L}} t'}\,\bar{\theta}_{L\max}$, one obtains the following formula for the normalized mean value temperature response of the layer:

$$\frac{\bar{\theta}_{\mathrm{L}}(t)}{\bar{\theta}_{L\max}} = 1 + \left(\frac{(\rho C_p K)_{\mathrm{S}}}{(\rho C_p K)_{\mathrm{L}}}\right)^{\frac{1}{2}} \left[\left(\frac{t_{\max}}{t'} - 1\right)^{\frac{1}{2}} \frac{\bar{\theta}_{\mathrm{S}}(t_{\max})}{\bar{\theta}_{L\max}} - \left(\frac{t}{t'} - 1\right)^{\frac{1}{2}} \frac{\bar{\theta}_{\mathrm{S}}(t)}{\bar{\theta}_{L\max}}\right] \tag{11}$$

Despite the fact that the above formula is quite difficult for practical use (since the terms in the square brackets may not be readily available), this equation indicates that the normalized mean value temperature response of the layer is a function of the ratio of the physical properties of the materials that make up the sample, i.e., $(\rho C_p K)_{\mathrm{S}}/(\rho C_p K)_{\mathrm{L}}$. For simplicity, this ratio will be referred to hereafter as $\Phi$. It is clear that for highly conductive layers the normalized temperature response of the sample surface (which is what the TTR method detects) would behave in a similar way as the normalized mean value response, $\bar{\theta}_{\mathrm{L}}(t)/\bar{\theta}_{L\max}$. In such cases, one discovers that a non-dimensional parameter, $\Phi$, governs the heat transfer problem in the finite layer. Indeed, in such a situation the mean temperature of the highly conductive layer is almost equal to the surface temperature, $\bar{\theta}_{\mathrm{L}}(t) \approx \theta(t,0)$. The evaluation of the applicability of this discovery to a wider range of material combinations (in which the properties ratio, $\Phi$, can be used as a governing parameter in the performance evaluation of the TTR method) is an important and potentially very useful result that will be examined in detail in the remainder of this article.

Table 3
Properties of the samples utilized in the comparison computations

| Sample | Materials | $\rho C_p$ (J/m$^3$ K) | $K$ (W/m K) | $h$ (Å) | $h/\delta_P$[a] | $(\rho C_p K)_S/(\rho C_p K)_L$ |
|---|---|---|---|---|---|---|
| 1 (Real) | Si substrate | $1.65\times10^6$ | 149 | 200,000 | 0.48 | 0.312 |
| | Au layer | $2.50\times10^6$ | 315 | 5,000 | | |
| 2 (Artificial) | Substrate | $3.30\times10^6$ | 49.7 | 200,000 | 0.48 | 0.312 |
| | Layer | $0.833\times10^6$ | 630 | 12,240 | | |

[a] $\delta_P$ was calculated for $\tau = 8.6$ ns, the pulse width in the SMU setup.

In addition to the ratio $\Phi$, the ratio of the layer thickness $h$ and the heat penetration depth during a pulse $\delta_P$ provides another dimensionless governing parameter ($h/\delta_P$) that is derived from the transient nature of the heat source (laser pulse) and the geometry of the sample. In order to confirm that the two aforementioned parameters are sufficient to entirely define the heat transfer process within a finite layer, we consider two samples, described in Table 3, that are entirely different but whose property ratios and dimensionless layer thicknesses are otherwise identical. The normalized temperature responses for the two samples, shown in Fig. 4(a), were obtained with the numerical simulation technique described previously in the heat transfer modeling section. As evident in Fig. 4(a), the normalized temperature responses of the samples match perfectly despite the differences in their material properties and layer thicknesses. This result proves that the temperature response is a function of only the properties ratio, $\Phi$, and the non-dimensional layer thickness, $h/\delta_P$.

It is worth investigating at this point whether the same two governing parameters also completely define the behavior of the responsivity, $\mathrm{Rs} = K(\mathrm{d}\widetilde{\Theta}(T)/\mathrm{d}K)_{\max}$, which was introduced earlier for a semi-infinite layer sample. The TTR method can measure the thermal conductivity of one unknown material at a time. In the case of a layer and a substrate, the thermal conductivity of either material can be determined as long as the other one is known. However, the responsivity of measuring the thermal conductivity of the layer need *not* be the same as that associated with measuring the substrate. To check this suspicion, the responsivity curves for the two samples in Table 3 were obtained as a function of the non-dimensional thickness of the layer and plotted in Fig. 4(b). Since there are two materials making up each sample and since, as previously mentioned, the TTR system can provide the thermal conductivity of only one material at a time, four curves are obtained. The results presented in Fig. 4(b) correspond to the cases where $K$ of the substrate material is under test (thin lines) or where $K$ of the layer is under test (bold lines). Analysis of the results shows that a different responsivity curve is obtained depending on the case considered, i.e., whether the layer or the substrate is the unknown. However, for each case, the responsivity curves of the two samples (Table 3) are perfectly matched within the range of the given layer thickness, proving again that the heat transfer process in a finite layer is governed only by the two non-dimensional parameters introduced above.

The results in Fig. 4(b) also indicate that a maximum responsivity is possible for a specific layer thickness, irrespective of which material is under test. This is an important discovery since the main interest of this investigation is to maximize the responsivity of the TTR

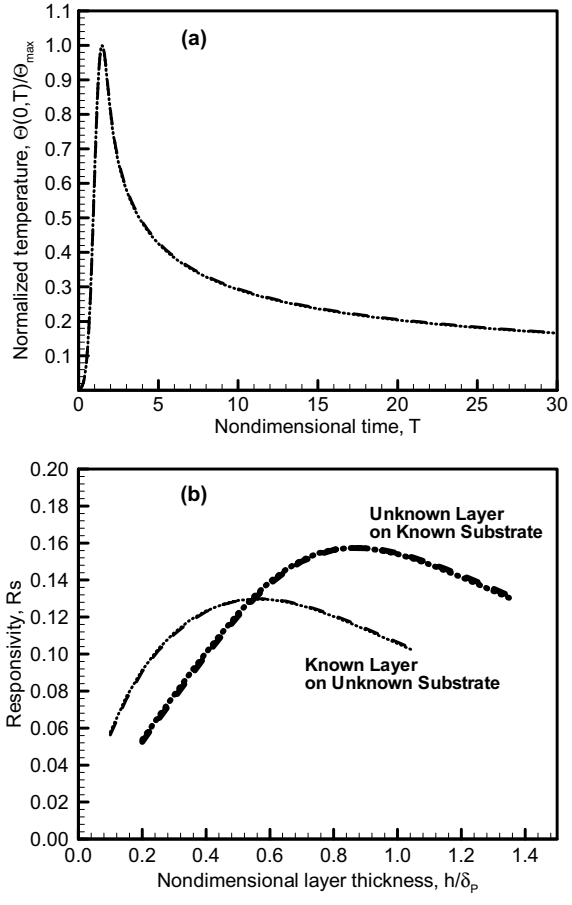


Fig. 4. Comparison of sample 1 (dotted) and sample 2 (dashed) having different properties and geometry, but same values of $\Phi$ and $h/\delta_P$ (Table 3): (a) temperature responses, and (b) measurement responsivity.

measurements for given materials and measurement system design. But, the existence of a maximum at a specific non-dimensional layer thickness also suggests that the maximum value of the responsivity and the optimal thickness of the layer (at which the maximum value occurs) are a function of the single similarity parameter $\Phi$. It is important to determine next the range of property values for which the previous proven hypothesis holds true. Since this problem represents a four dimensional parameter space ($\rho C_p$ and $K$ for both layer and substrate), it is impractical to consider all possible combinations of layer and substrate material properties by varying one single parameter at a time. Rather, it was decided to follow a more practical and equally predictive two-step process. First, select a representative conductive layer (which would be expected to comply with the hypothesis) and investigate the broad range of substrate material properties. Then, use a Monte Carlo type approach to randomly select combinations of layer and material properties and determine if the resulting data fit the behavior obtained in the first step. Inherent in this logic is the potential for discovery of the ranges of material properties where the resulting behavior would either obey or deviate from the single parameter similarity solution, which is the desired outcome of this investigation.

Hence, a conductive layer material in the mid-range of metals was chosen as a reference with $(\rho C_p)_L = 2.5 \times 10^6$ J/m$^3$ K and $K_L = 100$ W/m K. Then, the substrate material specific heat, $(\rho C_p)_S$, was varied within the range $-0.5 \leqslant \log((\rho C_p)_S/(\rho C_p)_L) \leqslant 1.0$, with a logarithmic step of 0.1, while the substrate material thermal conductivity, $K_S$, was varied within the range $-3.0 \leqslant \log(K_S/K_L) \leqslant 1.0$, with a logarithmic step of 0.1. As expected, the computational data resulting from the 656 simulations were found to collapse into lines within an uncertainty of less than 1%. In Fig. 5(a), the data obtained for the case when the substrate material is unknown are shown as solid and dashed lines for $Rs_{max}$ and $h_{max}/\delta_P$, respectively (the symbols will be discussed in a later section). Fig. 5(b) shows similar data for the case when the layer material is unknown. The existence of a single line fit strongly confirms the existence of the universal behavior, i.e., that the heat transfer problem is governed by the single parameter $\Phi$.

The second step in the two-step process is to check whether this apparent universal behavior is true for other highly diffusive materials. As previously discussed, repeating the investigation for a large number of layer materials would be impractical given the considerable number of computations for different values of $\Phi$ that would need to be run for each choice of layer material. Instead, by randomly choosing an appropriately large number of combinations of the four properties that make up each $\Phi$ value, it would be possible to cover the full spectrum of useful $K$ and $\rho C_p$ ranges. Consequently,

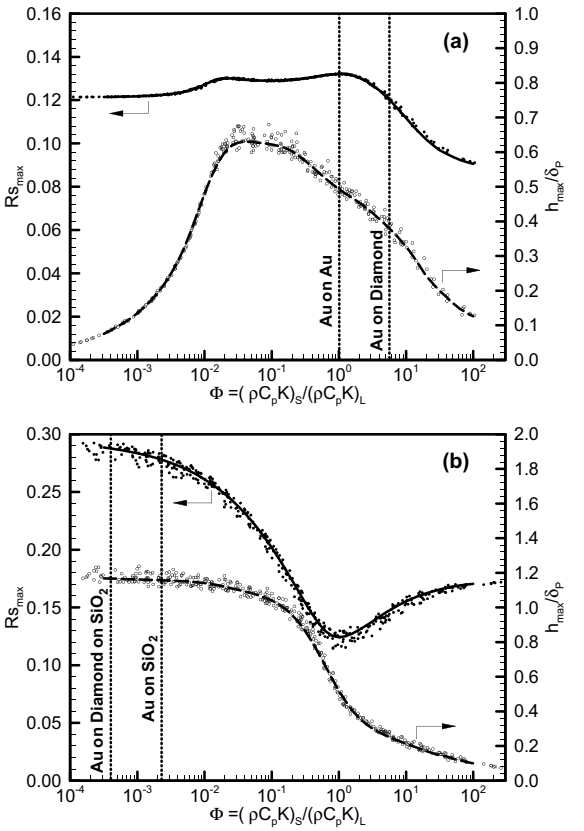


Fig. 5. Maximum responsivity and corresponding optimal layer thickness versus $\Phi$: (a) substrate is material under test; and (b) layer is material under test.

the investigation was performed for 1000 different random combinations of values of $K \in [0.1, 1000]$ W/m K and $\rho C_p \in [0.8 \times 10^6, 25 \times 10^6]$ J/m$^3$ K. Examination of the results revealed that data obtained from cases where the diffusivity of the layer is greater than $5 \times 10^{-6}$ m$^2$/s fall right on the (solid and dashed) lines in Fig. 5(a) and (b), while data obtained from cases where the layer is less diffusive deviate drastically from the single parameter similarity solutions. The data for $\alpha > 5 \times 10^{-6}$ m$^2$/s are superimposed as symbols on Fig. 5(a) and (b). The uncertainty envelopes for the responsivity and optimal thickness curves were ±5% and ±7%, respectively.

In conclusion, the above analysis confirms the discovery of the existence of a universal behavior of the maximum responsivity and the optimum layer thickness that depends only on the single variable $\Phi = (\rho C_p K)_S/(\rho C_p K)_L$ over a wide range of substrate material properties and a diffusivity-limited range of layer material properties. It should be pointed out, however, that the lower limit of $\alpha = 5 \times 10^{-6}$ m$^2$/s includes the entire range of metals used in microelectronics.

Before examining the implications of the above discovery on the optimization of the TTR method, the

results of Fig. 5 are described in more detail. Consider first the responsivity behavior of a substrate material under test (Fig. 5(a)). The maximum responsivity deviates around a mean of 0.125 within almost the entire investigated range of material properties ratio. The exception occurs at ratio values above 1, when the maximum responsivity goes down monotonically to $\sim$0.09 at $\Phi = 100$. The corresponding data of the optimal layer thickness vary more dramatically. The curve has a plateau within the range of 0.01–0.1, and decreases in both directions outside of this range, but more sharply at lower values of $\Phi$. It is worth mentioning that the optimal layer thickness never exceeds the heat penetration depth during a pulse, $\delta_P$.

Consider next the responsivity behavior when the layer material is unknown (Fig. 5(b)). The responsivity curve has a minimum value when the $\rho C_p K$ product is the same for both substrate and layer materials, i.e., $\Phi = 1$. At this point, the value of the responsivity is identical to the maximum value obtained for an unknown substrate material (Fig. 5(a)). From this minimal value the curve increases in either direction, with the maximum responsivity reaching significant values as high as 0.29, which is more than twice the maximum observed in the case of a semi-infinite layer sample (Fig. 3(a)). For small values of the material properties ratio ($\Phi < 1$), the optimal thickness also increases and even surpasses the heat penetration depth value, $\delta_P$, at $\Phi = 0.2$. Increasing $\Phi$ above unity causes the responsivity to increase and the optimal thickness to decrease. After comparison of the above cases, it is possible to conclude that the TTR measurement of the conductivity of a layer material is more accurate than the measurement of a substrate material. Indeed, the maximum responsivity values of the former case exceed those of the latter case in all of the explored range of $\Phi$. For small values of $\Phi$, the advantage can be by more than a factor of 2.

To conclude this article, three examples are given briefly to demonstrate the usefulness of the results. The first attempts to anticipate a potential question regarding the interesting material combination where both the layer and the substrate are made up of the same material, i.e., when $\Phi = 1$. Specifically, what should be expected when a finite layer of gold is deposited on a bulk gold substrate. From the finite layer approach described above, the expected measurement responsivity for the thin layer of gold should be 0.13 (Fig. 5(a)), which is sufficiently high. Fig. 6(a) presents the normalized temperature response of the gold sample along with the responses obtained by varying the conductivity of the substrate by ±20%. The observed deviation of the response corresponds to the normal appropriate sensitivity of the TTR method (see, e.g., [15]).

However, given that both the layer and the substrate are made of gold, the aforementioned finite layer sample

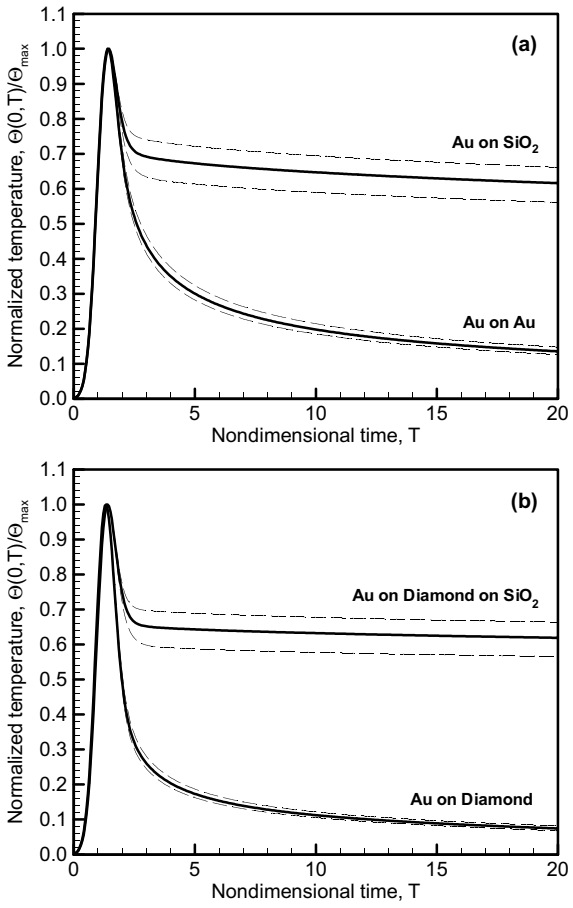


Fig. 6. Normalized temperature responses (solid lines) with ±20% deviation bands (dashed lines): (a) gold-on-gold and gold-on-silicon-dioxide samples; (b) gold-on-diamond and gold-on-diamond-on-silicon-dioxide samples.

can be treated as a semi-infinite layer sample. If treated as such, the *Fo* number would be on the order of a thousand, which would result in a measurement responsivity of approximately zero (Fig. 3(a)). At first glance, this situation is paradoxical since for the same exact sample, a TTR measurement is impossible from one perspective while from another the measurement is not only possible but can be done with an appropriate level of accuracy. The apparent paradox can be simply resolved by realizing that in the semi-infinite layer treatment only one material can be handled (the one whose thermal conductivity needs to be measured). In the finite layer treatment there are two materials (layer and substrate), even if they are chemically identical, and only the conductivity of the substrate material is varied in the matching procedure of the TTR method since all properties of the layer material are supposed to be known. Thus, the sample accumulates the heating energy into the upper region whose properties are known and releases

that energy into the unknown material of the underlying substrate. Conversely, when the sample is treated as semi-infinite, both the accumulation and dissipation of the energy occur in the same material, whose thermal property is under test and hence is unknown. Consequently, it is not possible to extract the conductivity since the measurement problem is equivalent to a mathematical problem with a single equation and two unknowns.

The second example demonstrates another important outcome of this investigation; namely, that more accurate TTR measurements of a highly conductive material (e.g., gold) can be done if an optimal thickness of such a metal is deposited on a substrate of low and known conductivity (e.g., silicon dioxide). In such a case, the responsivity of the measurements can be doubled to 0.28 (Fig. 5(b)) by an appropriate choice of the thickness of the gold layer. Indeed, the temperature response of the optimal 1.2 μm gold layer deposited on a silicon dioxide substrate exhibits very high sensitivity as evident from the spread between the ±20% (dashed) curves in Fig. 6(a).

The third example illustrates how even superconductive materials like diamond can be measured successfully with a responsivity value of 0.12 (Fig. 5(a)), if the metallization layer covering it has an optimal thickness and well-known optical and thermal properties (e.g., gold). A responsivity value of 0.12 is sufficiently high as can be ascertained by examining Fig. 6(b) which presents the normalized temperature response of the gold-covered diamond sample bounded by the temperature responses obtained by varying the conductivity of the diamond by ±20%.

However, the results summarized in Fig. 5(b) indicate that more significant gains in the responsivity (of up to a value of 0.29) can be obtained by depositing a diamond layer with an optimal thickness on silicon dioxide, for example. Since diamond is a transparent material, a metallization layer (e.g., gold) is required on top of it in order to absorb the energy of the pulsed laser. The temperature response for the gold-covered diamond layer on an $SiO_2$ substrate is shown in Fig. 6(b) bounded by the responses associated with the ±20% deviation in the conductivity of diamond. Although the thickness of the gold layer in this example was chosen to be thin (500 Å) so as not to change the responsivity of the measurement, a more detailed analysis of its impact on the problem would be desirable. However, such an analysis would have to deal with two layers of different materials on the substrate, which is beyond the scope of the present work and part of a forthcoming investigation.

## 4. Conclusions

A one-dimensional analytical solution of heat transfer in a bulk, semi-infinite layer sample was derived in non-dimensional form in order to analyze the temperature response of the sample's surface. Most importantly, it was shown that the shape of the temperature response can be uniquely described by a single parameter, namely the *Fo* number. The analytical solution shows that the "amplitude" approach for extracting the thermal conductivity from experimental data leads to high uncertainty because of the necessity to obtain a calibration curve of temperature versus reflectivity. In contrast, the "shape" approach does not require prior calibration, and is therefore more attractive for thermal conductivity measurements.

On the basis of the analytical solution, it was also possible to determine both the responsivity of the TTR method and the measurement uncertainty of a particular TTR system. That, in turn, revealed the range of applicability of the "shape" method, namely, $Fo < 100$ for any TTR method and $Fo < 10$ for the particular TTR system used in the authors' laboratory. The TTR method provides the maximum accuracy for $Fo < 0.1$, which corresponds to a maximum responsivity value of $\mathrm{Rs}_{\max} = 0.125$. The introduction of the heat penetration depth ($\delta_{\mathrm{H}}$) of the laser pulse energy provides a basis for classifying a given sample that has a top layer whose thickness is larger than $\delta_{\mathrm{H}}$ as a semi-infinite layer sample. Specifically, the thickness of a semi-infinite layer should be at least seven times larger than the light penetration depth ($\delta_{\lambda}$) of the irradiation produced by the heating laser. Otherwise, the sample should be classified as a finite layer sample.

While the main approach to the heat transfer problem of a finite layer sample is numerical, a simplified analytical analysis of the problem has revealed two essential parameters, namely, the ratio of the physical properties of the materials that make up the sample, $\Phi = (\rho C_p K)_{\mathrm{S}}/(\rho C_p K)_{\mathrm{L}}$, and the dimensionless layer thickness, $h/\delta_{\mathrm{P}}$, which together entirely define the behavior of the normalized temperature response as well as the responsivity of the conductivity measurement. Since it was discovered that the responsivity, Rs, exhibits a maximum at a specific (optimal) layer thickness of a finite layer sample, it becomes possible to tie the maximum responsivity, $\mathrm{Rs}_{\max}$, and the optimal thickness, $h_{\max}/\delta_{\mathrm{P}}$, to the properties ratio, $\Phi$, for both cases when the layer material or the substrate material are under test. For each case, two universal relationships were obtained relating $\mathrm{Rs}_{\max}$ and $h_{\max}/\delta_{\mathrm{P}}$ to $\Phi$ over wide ranges of specific heat values, $\rho C_p \in [0.8 \times 10^6, 25 \times 10^6]$ J/m$^3$ K, and thermal conductivity values, $K \in [0.1, 1000]$ W/m K. It was determined that the applicability of those relationships is limited by the inequality $K/\rho C_p > 5 \times 10^{-6}$ m$^2$/s for the layer properties, which nevertheless covers the range of useful microelectronics materials.

The main conclusion of the findings associated with finite layer samples is that the TTR measurement performance (maximum responsivity) is higher if the material under test is a layer rather than a substrate. For

example, the use of diamond as a layer on a silicon dioxide substrate (with thin gold metallization for the light absorption) increases the measurement accuracy by a factor of two as compared with the case where the diamond is a substrate covered by an optimal layer of gold.

## References

[1] The National Technological Roadmap for Semiconductors, International Sematech Corporation. Available from http://www.sematech.org/public/publications/index.htm; http://public.itrs.net.
[2] D.G. Cahill, Heat transport in dielectric thin films and at solid–solid interfaces, in: C.L. Tien, A. Majumdar, F.M. Gerner (Eds.), Microscale Energy Transport, Taylor and Francis, Washington, DC, 1998, pp. 95–117.
[3] A. Majumdar, Microscale heat conduction in dielectric thin films, ASME J. Heat Transfer 115 (1993) 7–16.
[4] W.S. Capinski, H.J. Maris, Improved apparatus for picosecond pump-and-probe optical measurements, Rev. Scientific Instrum. 67 (1996) 2720–2726.
[5] D.Y. Tzou, Macro- to Microscale Heat Transfer (The Lagging Behavior), Taylor and Francis, Washington, DC, 1997, Ch. 1.
[6] I. Hatta, Thermal diffusivity measurements of thin films and multilayered composites, Int. J. Thermophys. 11 (1990) 293–303.
[7] X. Xu, C.P. Grigoropoulos, R.E. Russo, Transient temperature during pulsed excimer laser heating of thin polysilicon films obtained by optical reflectivity measurement, ASME J. Heat Transfer 117 (1995) 17–24.
[8] T.Q. Qiu, C.L. Tien, Femtosecond laser heating of multilayer metals—I. Analysis, Int. J. Heat Mass Transfer 37 (1994) 2789–2798.
[9] G. Chen, C.L. Tien, X. Wu, J.S. Smith, Thermal diffusivity measurement of GaAs/AlGaAs thin-film structures, ASME J. Heat Transfer 116 (1994) 325–331.
[10] T.Q. Qiu, C.L. Tien, Heat transfer mechanisms during short-pulse laser heating of metals, ASME J. Heat Transfer 115 (1993) 835–841.
[11] H.C. Carslaw, J.C. Jaeger, Conduction of Heat in Solids, second ed., Clarendon Press, Oxford, 1959.
[12] A. Paddock, G.L. Eesley, Transient thermoreflectance from thin metal films, J. Appl. Phys. 60 (1986) 285–290.
[13] N. Ozisik, Boundary Value Problems Of Heat Conduction, Dover Publications, Inc, New York, 1989.
[14] C.A.J. Fletcher, Computational Techniques fir Fluid Dynamics, second ed., vol. 1, Springer-Verlag, New York, 1991, p. 229.
[15] O.W. Kading, H. Skurk, K.E. Goodson, Thermal conduction in metallized silicon-dioxide layers on silicon, Appl. Phys. Lett. 65 (1994) 1629–1631.
[16] E.D. Palik (Ed.), Handbook of Optical Constants of Solids, Academic Press, San Diego, 1998.